Supplementary Information (SI) for Journal of Materials Chemistry B.

H_2O_2 Responsive Rhodamine-Based Probe for Monitoring Early-Stage Diabetes Diagnosis

Moumita Mondal,[a, b] Pravat Ghorai,[a] Asmita Samadder,[c] Stefan A. Freunberger,*[d] Priyabrata Banerjee *[a, b]

a. Electric Mobility & Tribology Research Group, CSIR-Central Mechanical Engineering Research Institute, Mahatma Gandhi Avenue, Durgapur, 713209, India, E-mail: pbanerjee.cmeri@csir.res.in, priyabratabanerjee.chem@gmail.com; Tel: +91-9433814081

b. Academy of Scientific & Innovative Research (AcSIR), Ghaziabad-201002, Uttar Pradesh, India

c. Cytogenetics and Molecular Biology Laboratory, Department of Zoology, University of Kalyani, Kalyani, Nadia-741235, India

d. Institute of Science and Technology Austria (ISTA), Am Campus 1, 3400 Klosterneuburg, Austria, E-mail: Stefan.Freunberger@ist.ac.at

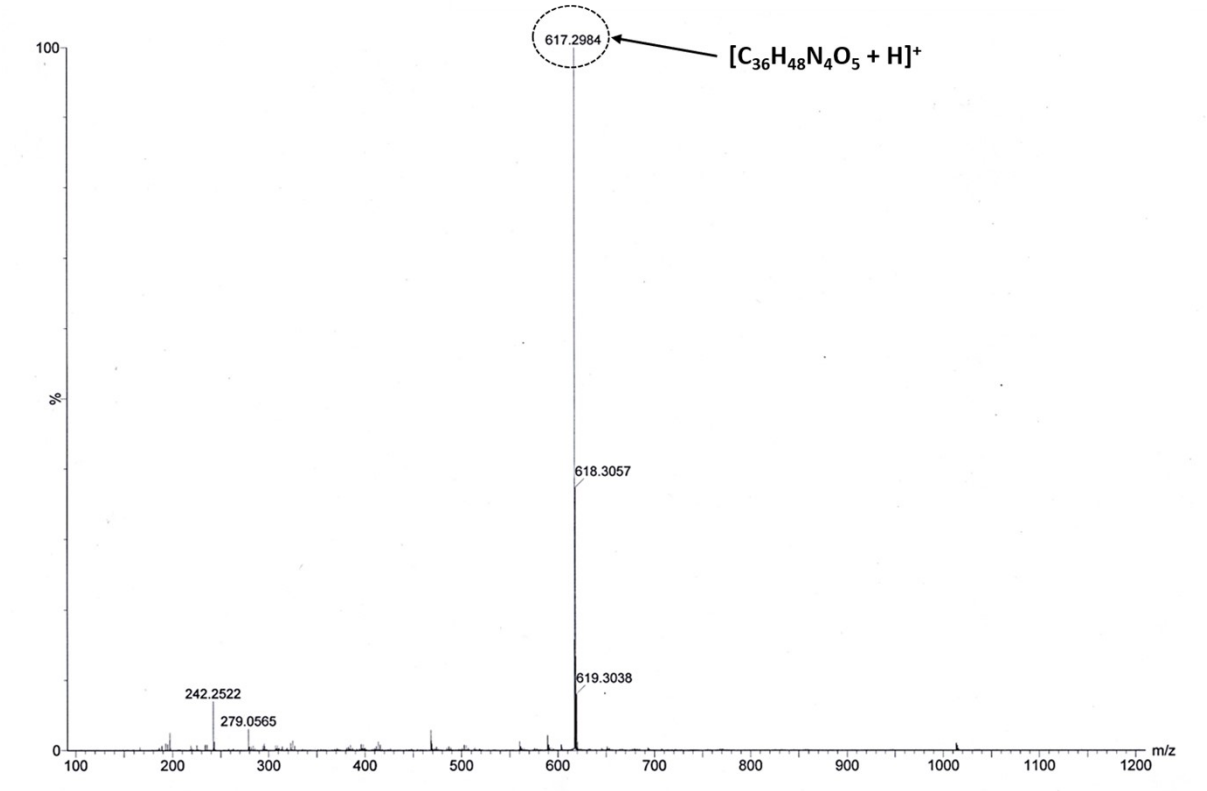

Figure S1: ESI-MS spectrum of the synthesized sensory probe RN.

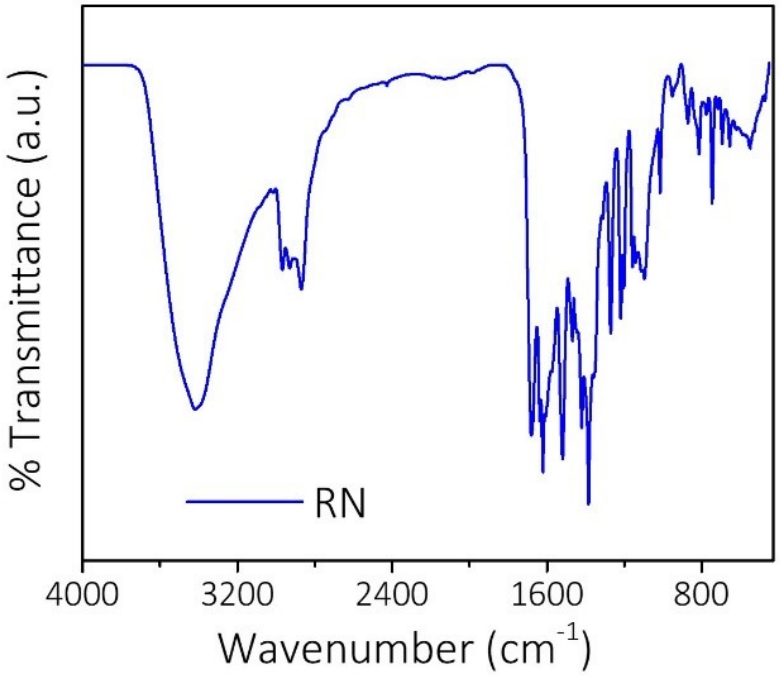

Figure S2: FT-IR (KBr pellet) spectrum of RN.

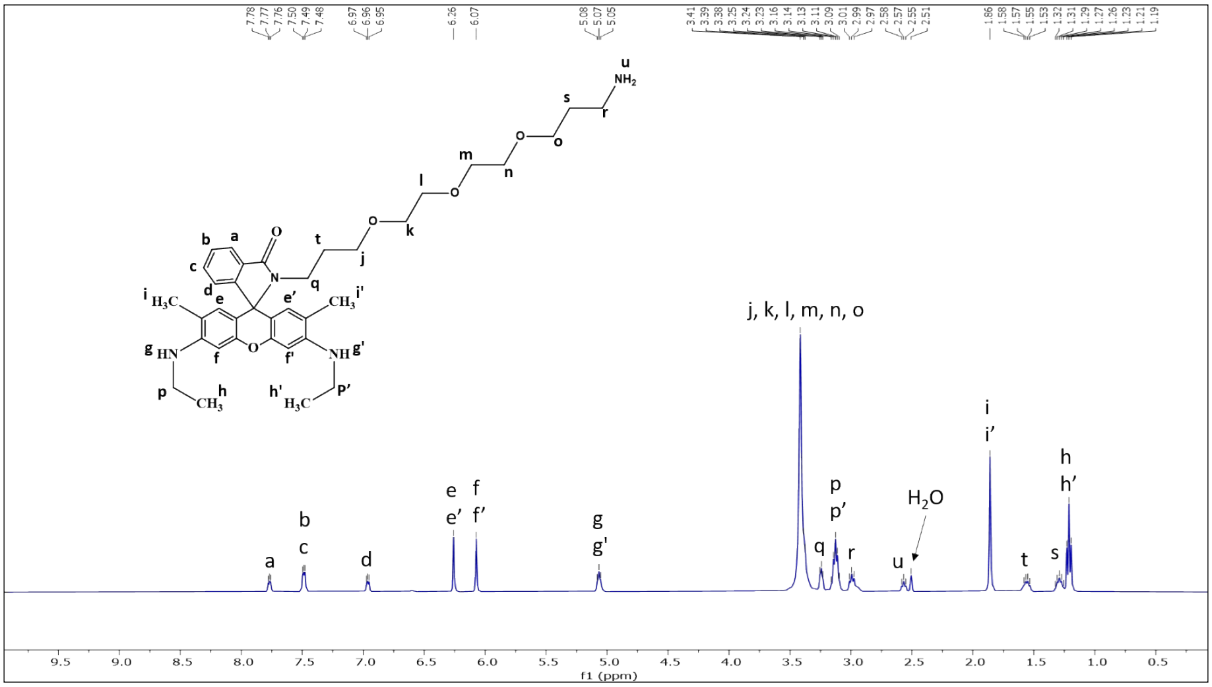

Figure S3: ^{1}H NMR spectrum of RN in DMSO-d_6 (400 MHz).

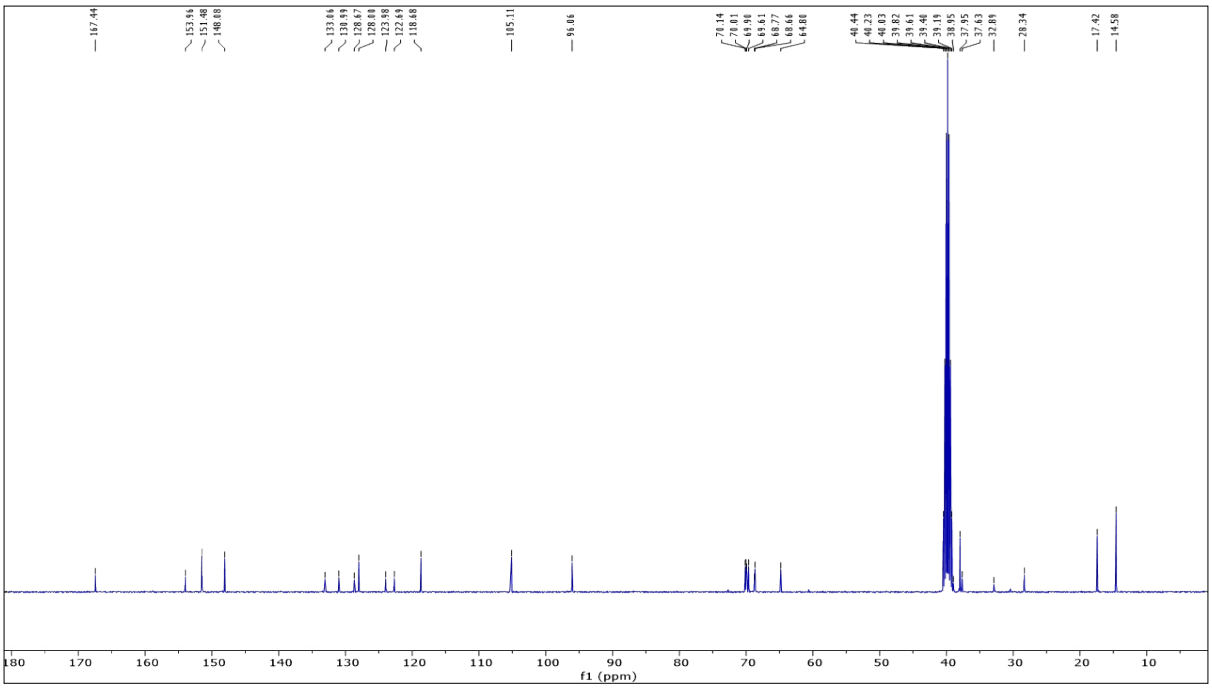

Figure S4: ^{13}C NMR spectrum of RN in DMSO-d_6 (400 MHz).

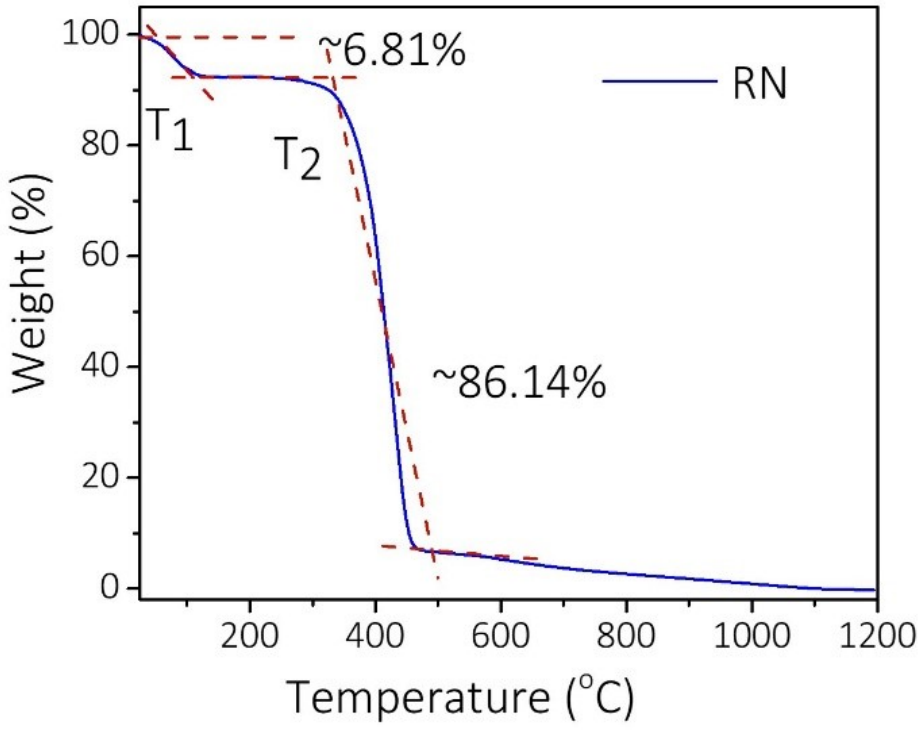

Figure S5: Thermogravimetric analysis (TGA) of RN.

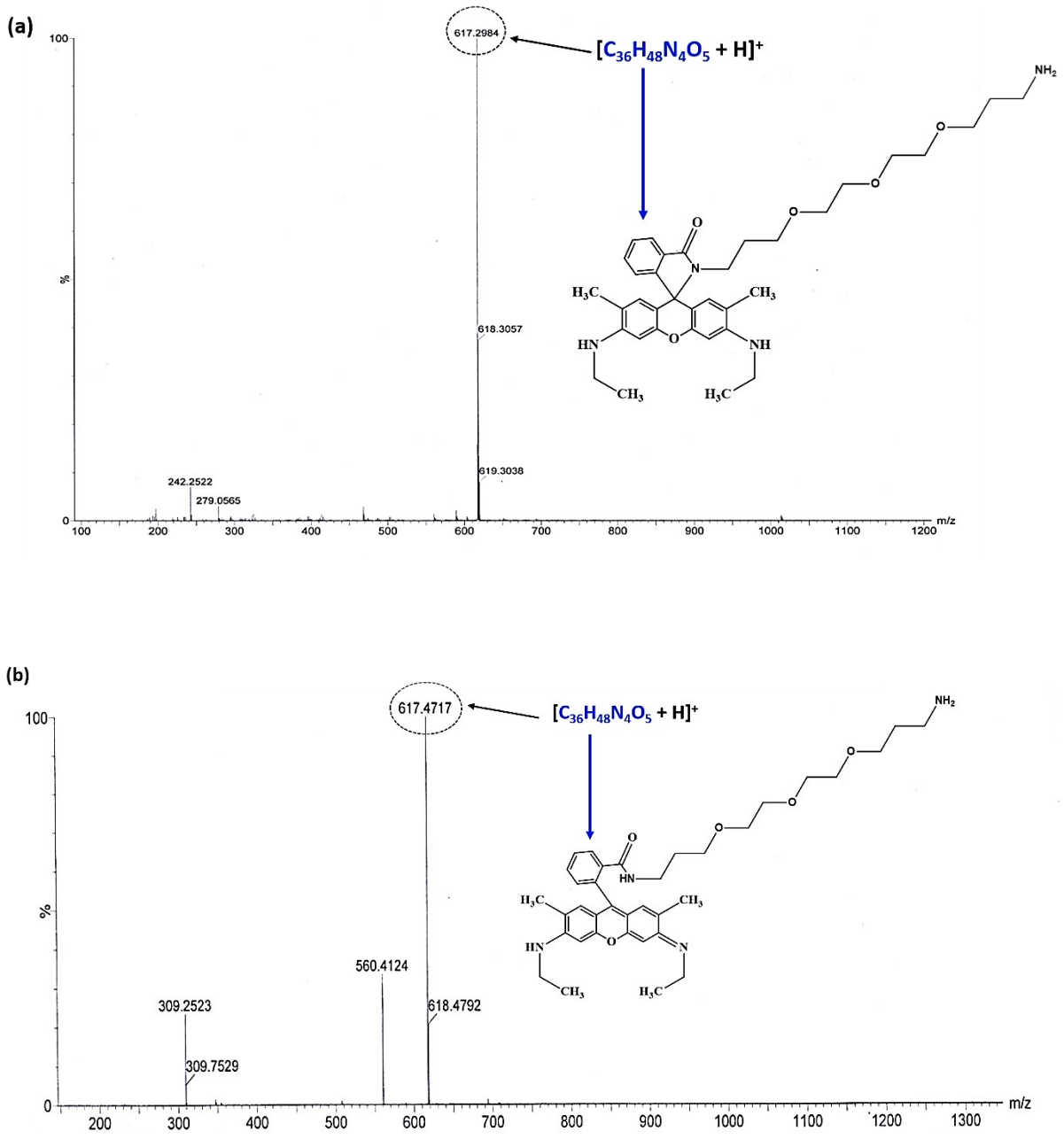

Figure S6: (a) ESI-MS spectrum of RN before H_2O_2 addition. (b) ESI-MS spectrum of RN after H_2O_2 addition.

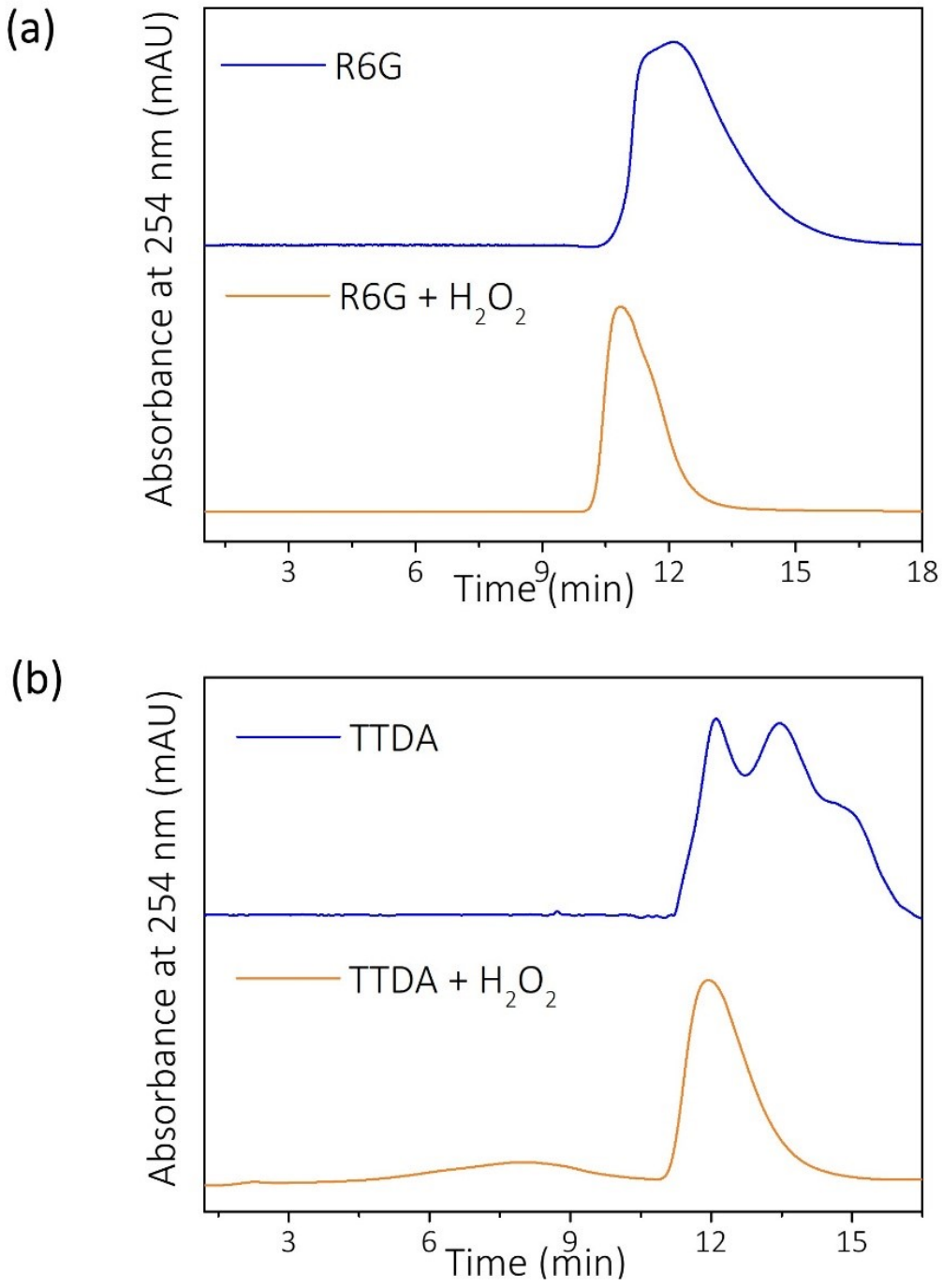

Figure S7: HPLC chromatograms of (a) R6G, and (b) TTDA with H_2O_2 addition (mobile phase water/methanol=70/30).

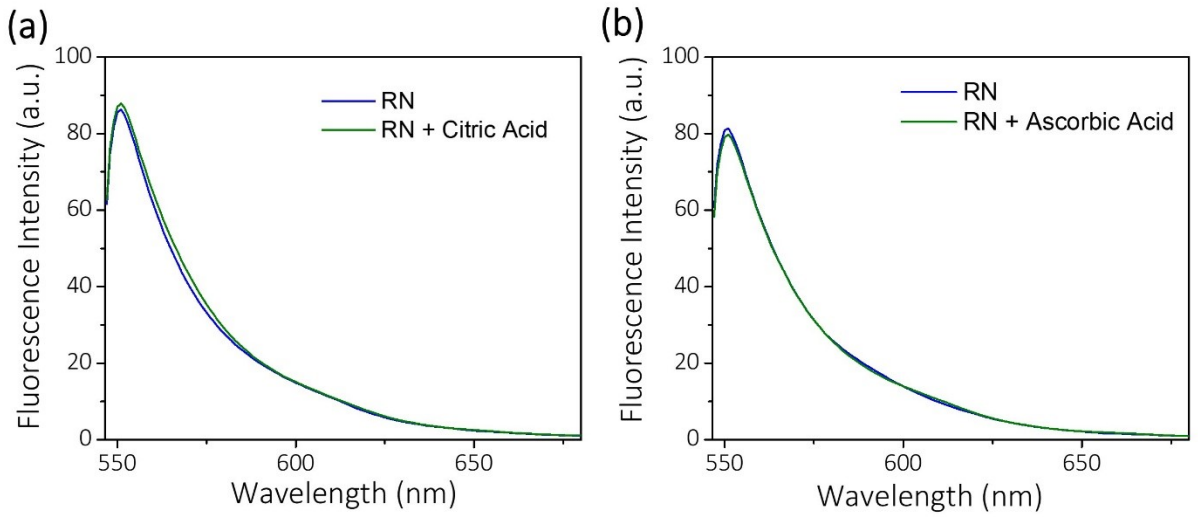

Figure S8: Response of RN in the presence of 1 mM of **(a)** Citric Acid (pH~ 2.98) and **(b)** Ascorbic acid (~3.5).

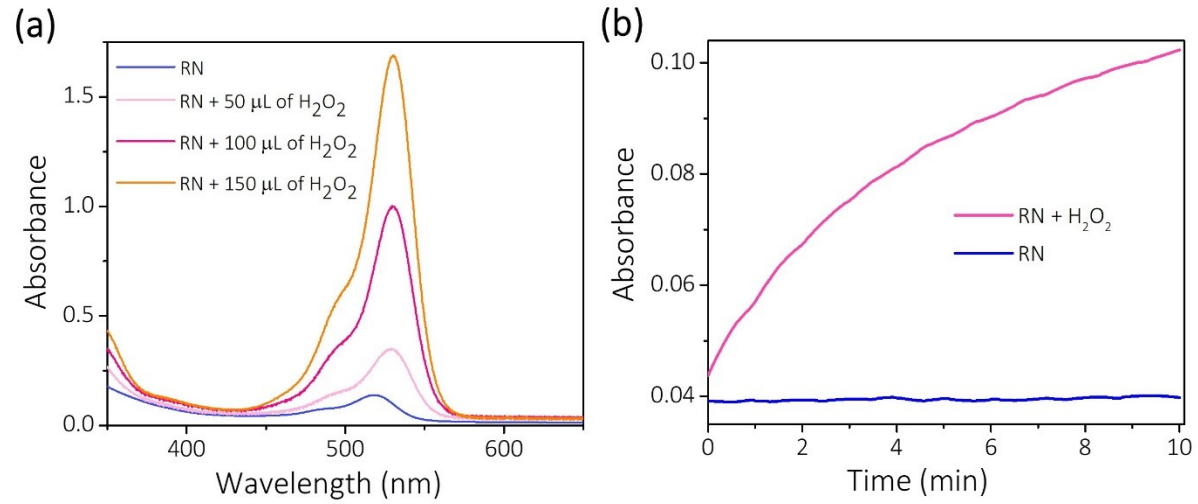

Figure S9: (a) UV-Vis spectra of RN after the addition of H_2O_2. **(b)** Effect of response time on the UV-Vis absorbance of RN at 525 nm at different time intervals.

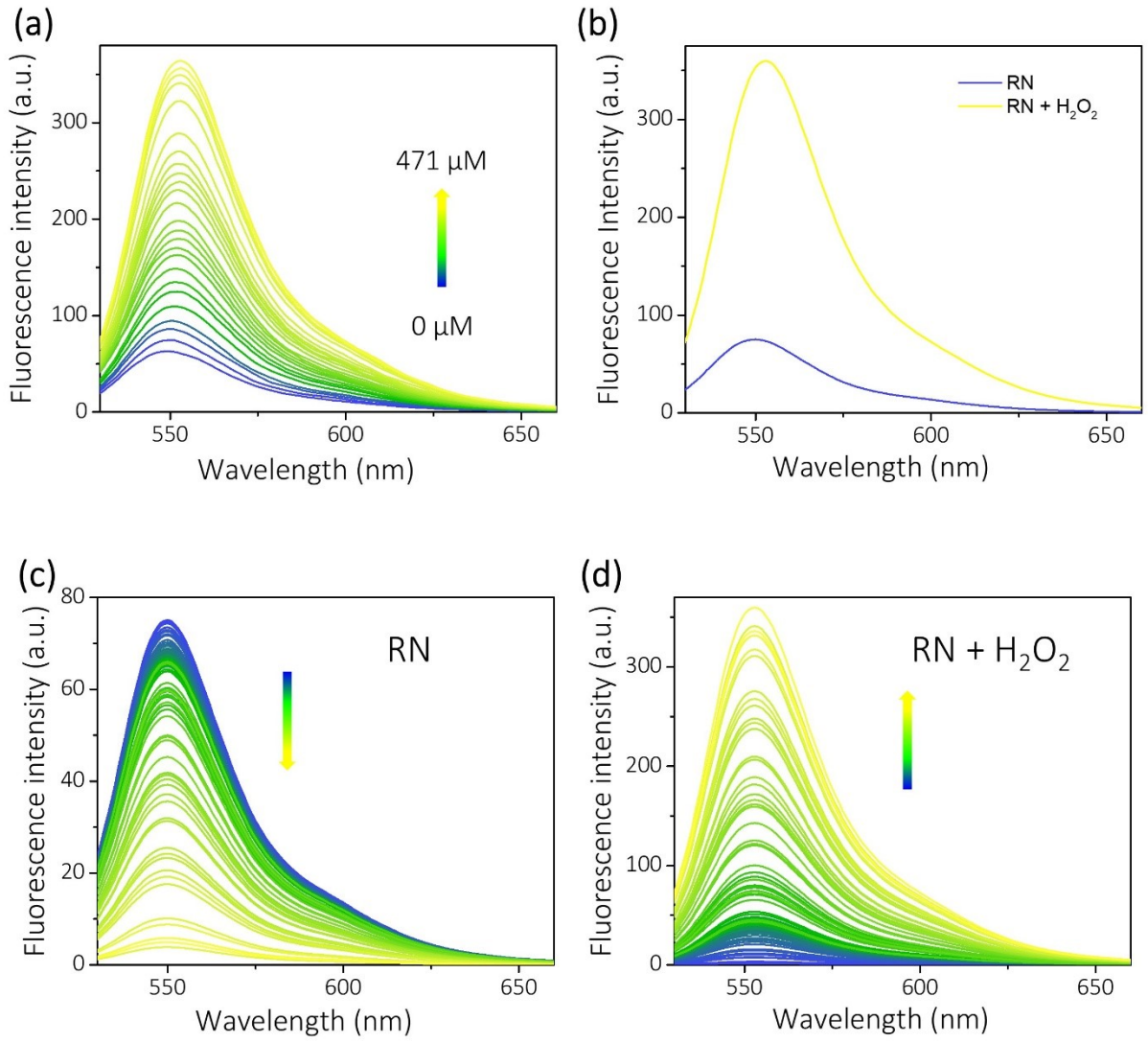

Figure S10: (a) Experimental data of fluorescence emission spectra of RN in the presence of different concentrations (0–471 µM) of H_2O_2 (λ_{ex}=520 nm). **(b)** Deconvoluted spectral plot of RN and RN + H_2O_2, showing ~5 nm peak shifting. Deconvoluted spectra of **(c)** RN and **(d)** RN + H_2O_2.

(Deconvolution method: multivariate curve resolution with evolving factor analysis with non-negative and total closure condition.)

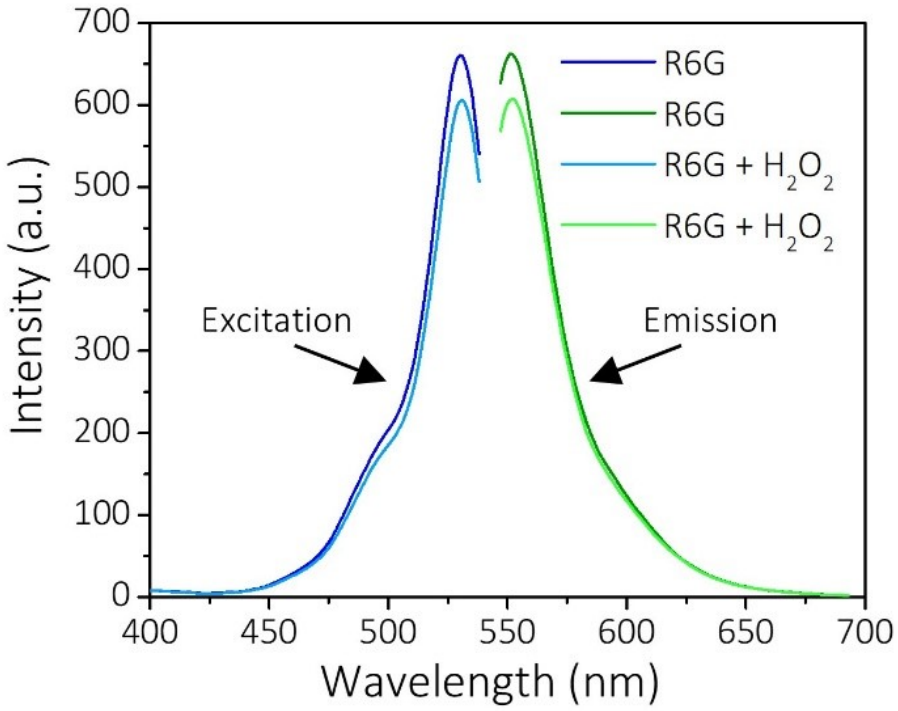

Figure S11: Excitation and emission spectra of R6G in ethanol after the addition of 1 mM of H_2O_2.

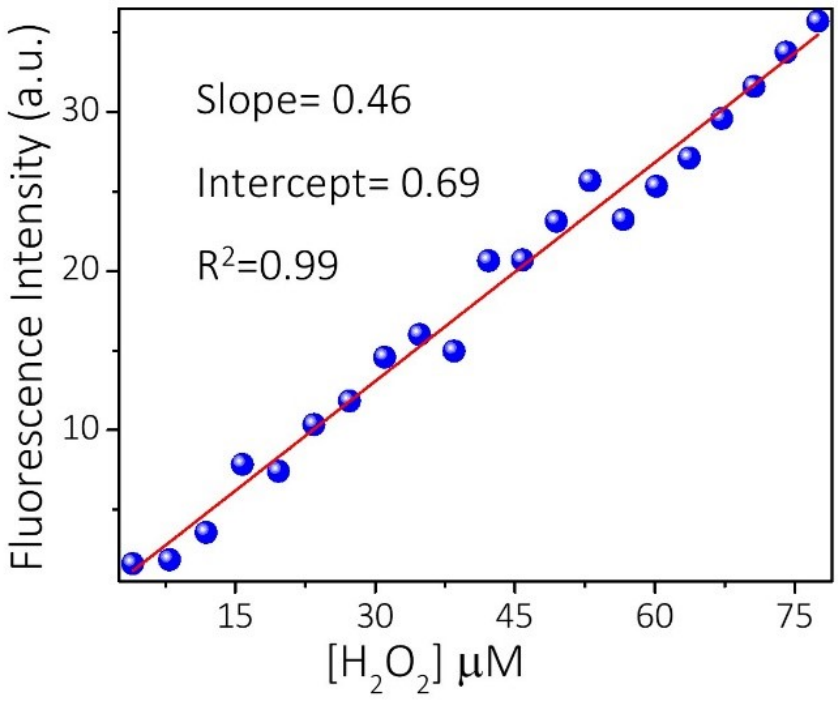

Figure S12: Deconvoluted fluorescence intensity of RN at 555 nm as a function of H_2O_2 concentrations (3.98–77.49 µM).

Preparation of reactive oxygen species (ROS):

Various ROS were prepared using the reported methods.[1–3] The preparation is briefly described below. All the solutions were freshly prepared every time and further diluted as per the requirements.

H_2O_2: The concentration of H_2O_2 was obtained based on the optical density at 240 nm with a molar extinction coefficient of 43.6 M^{-1} cm^{-1}. Then, the required concentration of H_2O_2 was prepared by appropriately diluting it with deionised water.

OCl^-: This solution was prepared by diluting sodium hypochlorite (NaOCl) appropriately in deionised water. The concentration of OCl^- was determined based on the optical density at 290 nm with molar extinction coefficient of 350 M^{-1} cm^{-1}.

NO_2^-: It was prepared by dissolving commercially available $NaNO_2$ in deionised water.

TBHP: It was prepared by diluting commercially available tert-butyl hydroperoxide (TBHP).

$OH^\bullet$: It was generated by the Fenton reaction by using the same concentration of iron sulfate ($FeSO_4$) solution and H_2O_2. The concentration of $OH^\bullet$ depends on the Fe^{2+} concentration.

$O_2^{\bullet-}$: It was prepared from potassium superoxide (KO_2)

$^1O_2$: It was generated in situ from ClO^- and H_2O_2.

$ONOO^-$: 0.6 M HCl was added to a reaction mixture of 0.6 M $NaNO_2$ and 0.6 M H_2O_2. Then 1.5 M of NaOH was added to it immediately. The concentration was determined based on the optical density at 300 nm with a molar extinction coefficient of 1670 M^{-1} cm^{-1}.

Calculation of Quantum yield

Quantum yields of RN in the absence and presence of H_2O_2 were estimated with respect to rhodamine 6G in ethanol as a standard. The concentrations of solutions used for the standard and RN were 10 µM. The fluorescence quantum yield (φ) has been calculated as follows[4]

$$\varphi_{sample} = \varphi_{reference} \times \frac{I_{reference}}{I_{sample}} \times \frac{A_{sample}}{A_{reference}} \times \frac{n_{sample}^{2}}{n_{reference}^{2}}$$

Where φ_{sample} is for the quantum yield of RN in the absence and presence of H_2O_2. $\varphi_{reference}$ is the quantum yield of standard and here the value is 0.95. I represents integrated intensities (areas) of

sample and standard spectra (in units of photons); A is the optical density and n stands for the refractive indices of the sample and reference solution.

The values of φ for RN in the absence and presence of H_2O_2 were estimated to be 0.142 and 0.457, respectively.

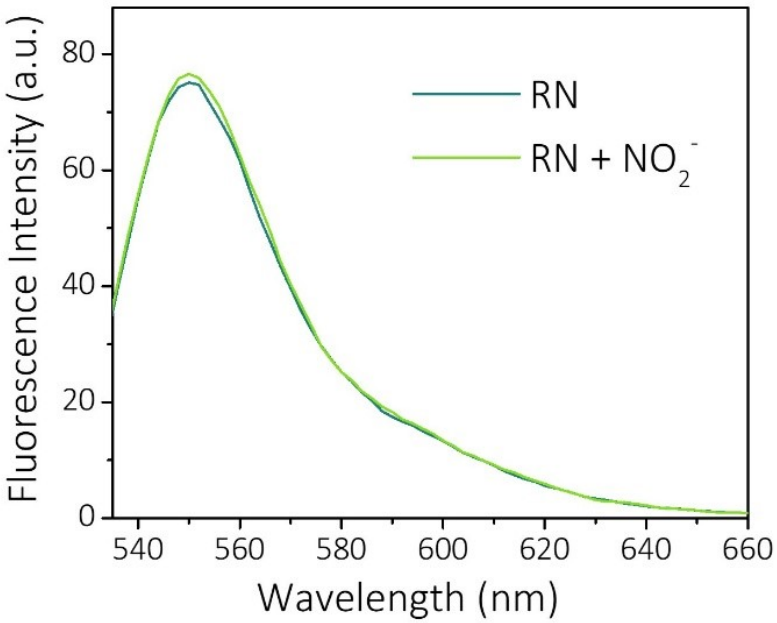

Figure S13: 1 mM of $NaNO_2$ solution was added to a solution of 10 µM of RN solution and the fluorescence intensity was measured to check the selectivity towards NO_2^-.

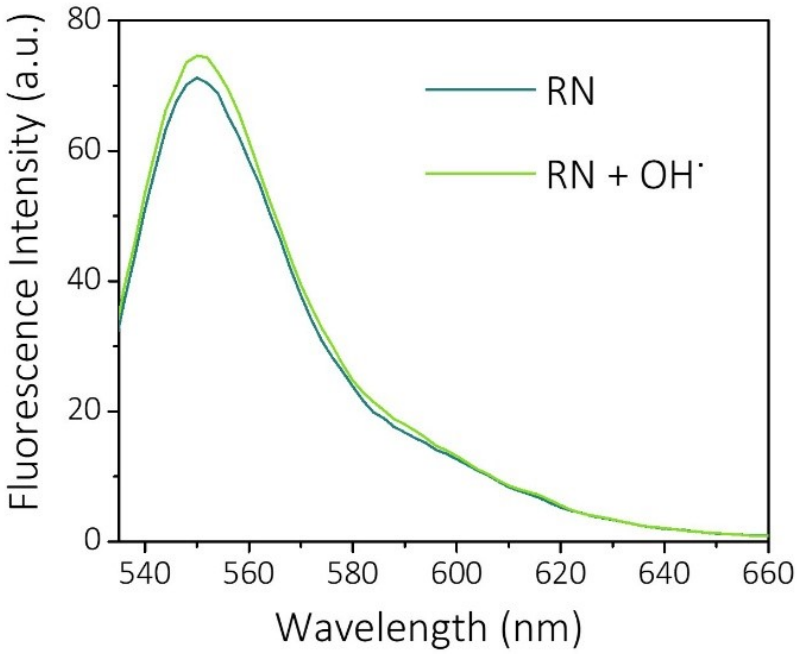

Figure S14: 1 mM of $OH^{\bullet}$ solution was added to a solution of 10 µM of RN solution and the fluorescence intensity was measured to check the selectivity towards $OH^{\bullet}$.

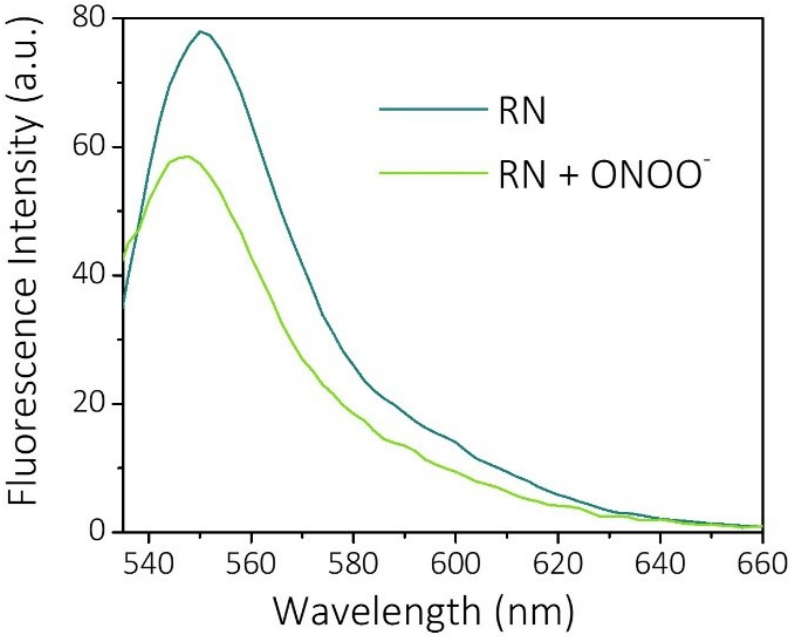

Figure S15: 1 mM of $ONOO^-$ solution was added to a solution of 10 µM of RN solution and the fluorescence intensity was measured to check the selectivity towards $ONOO^-$.

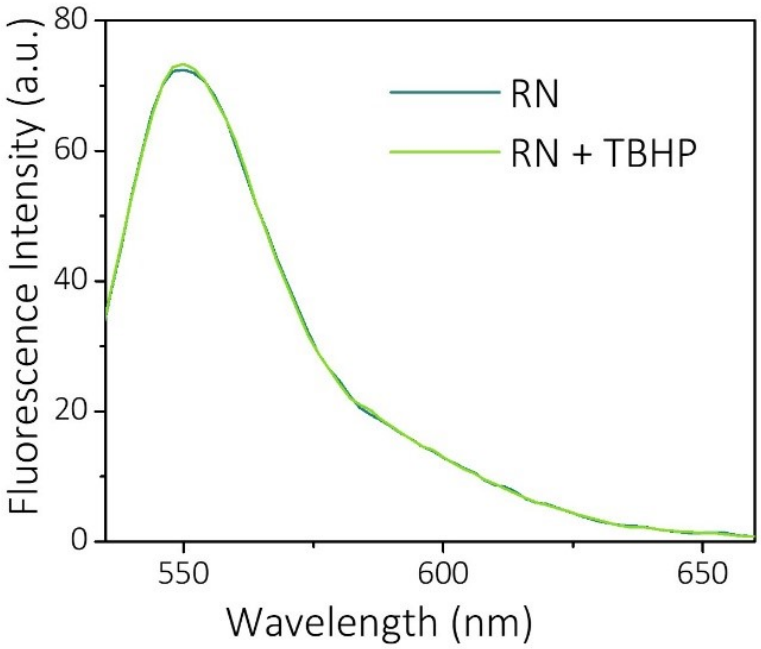

Figure S16: 1 mM of $ONOO^-$ solution was added to a solution of 10 µM of RN solution and the fluorescence intensity was measured to check the selectivity towards tert-Butyl hydroperoxide (TBHP).

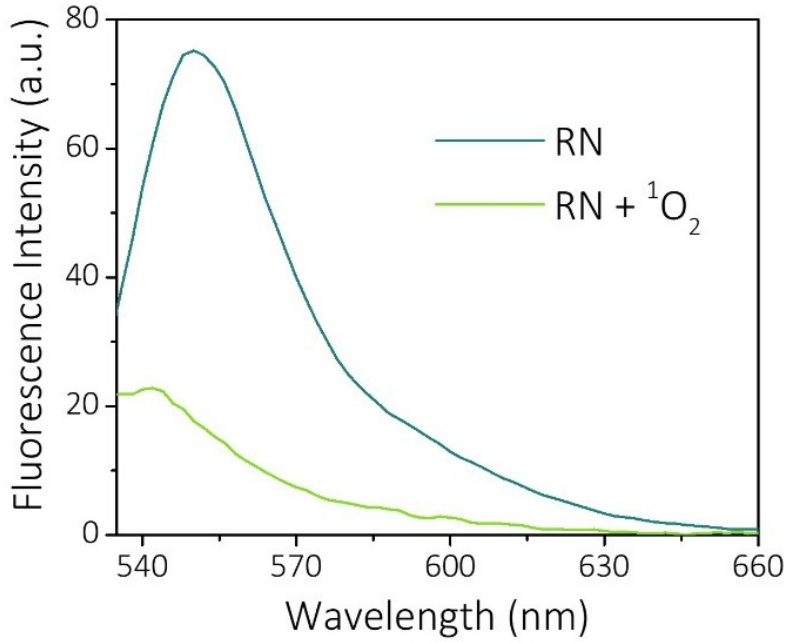

Figure S17: 10 µM of RN solution was added with $^1O_2$, generated from NaOCl and H_2O_2 and the fluorescence intensity was measured to check the selectivity towards $^1O_2$.

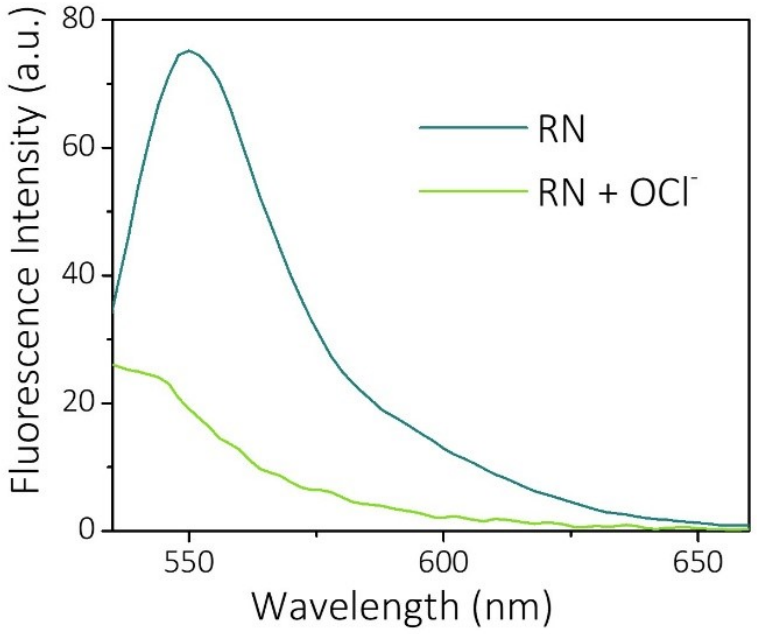

Figure S18: 1 mM of NaOCl solution was added to a solution of 10 µM of RN solution and the fluorescence intensity was measured to check the selectivity towards ClO^-.

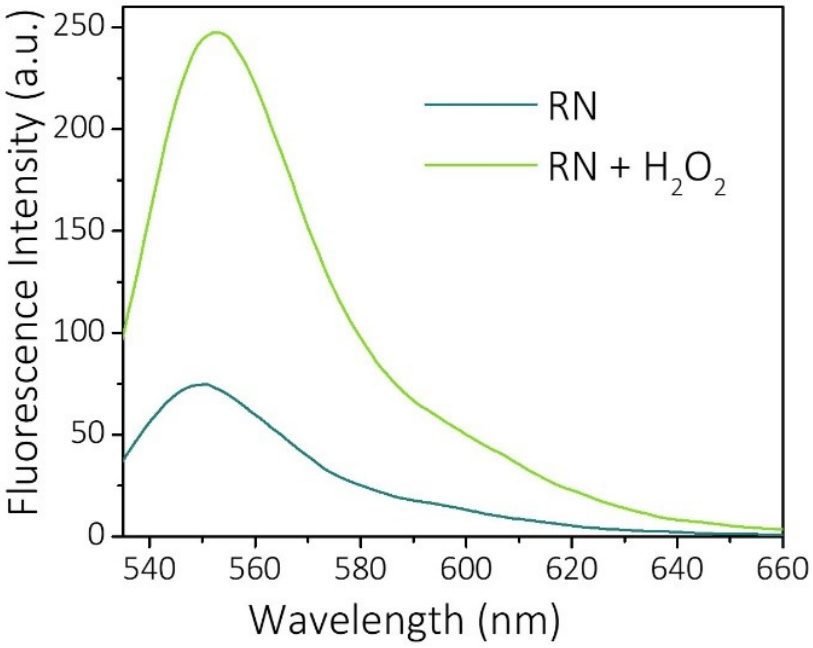

Figure S19: 1 mM of H_2O_2 solution was added to a solution of 10 µM of RN solution and the fluorescence intensity was measured towards H_2O_2.

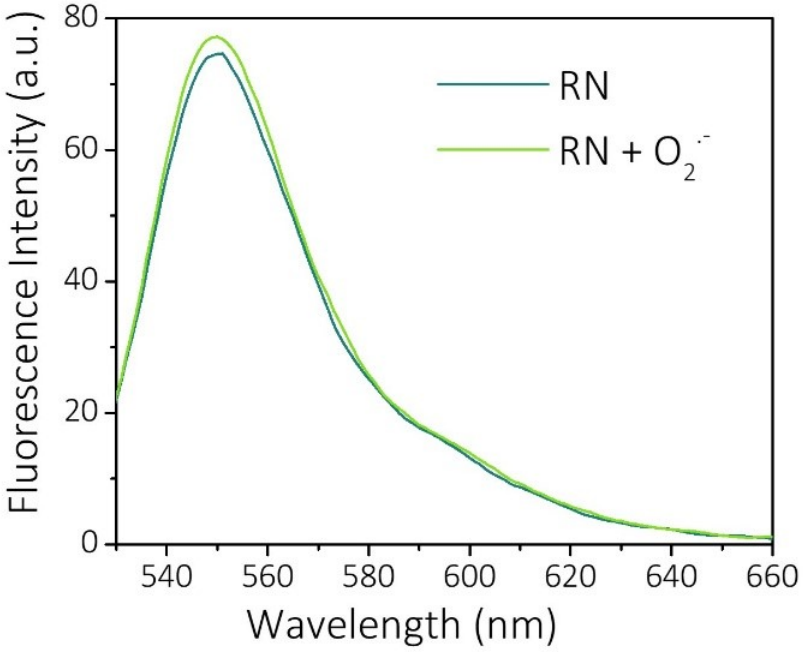

Figure S20: 1 mM of $O_2^{\cdot -}$ solution was added to a solution of 10 µM of RN solution and the fluorescence intensity was measured towards $O_2^{\cdot -}$.

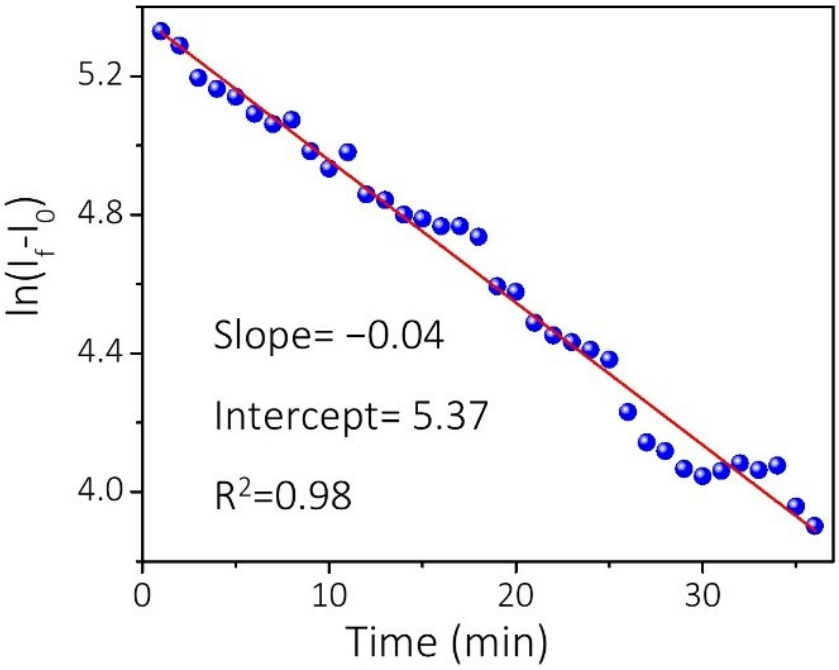

Figure S21: Determination of reaction rate constant following pseudo-first order kinetics.

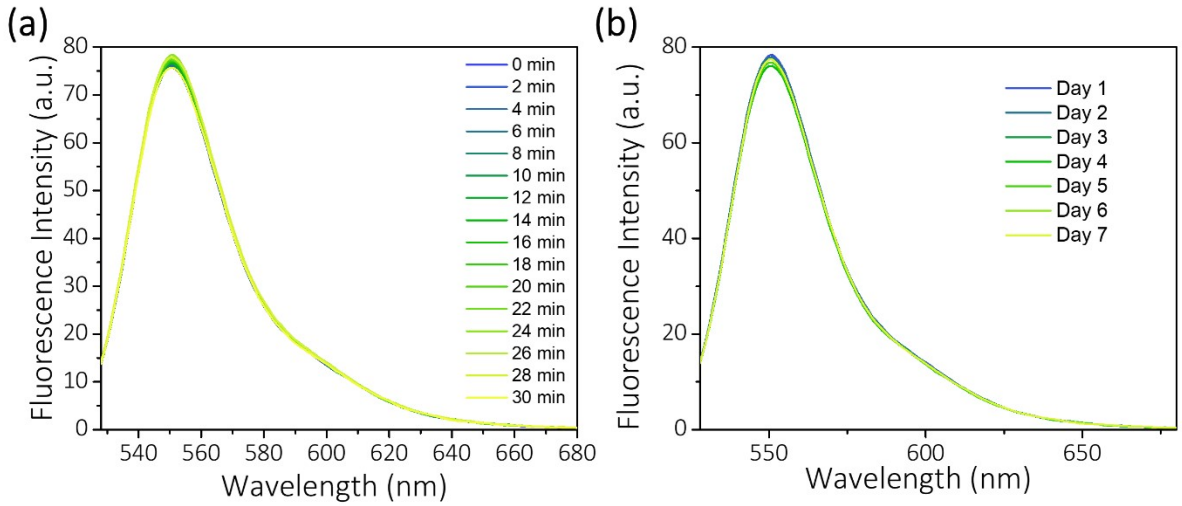

Figure S22: Time-dependent fluorescence emission profile of RN (10 µM RN in EtOH) for measuring the photostability: (a) RN over a period of 30 minutes, (b) RN over a period of 7 days.

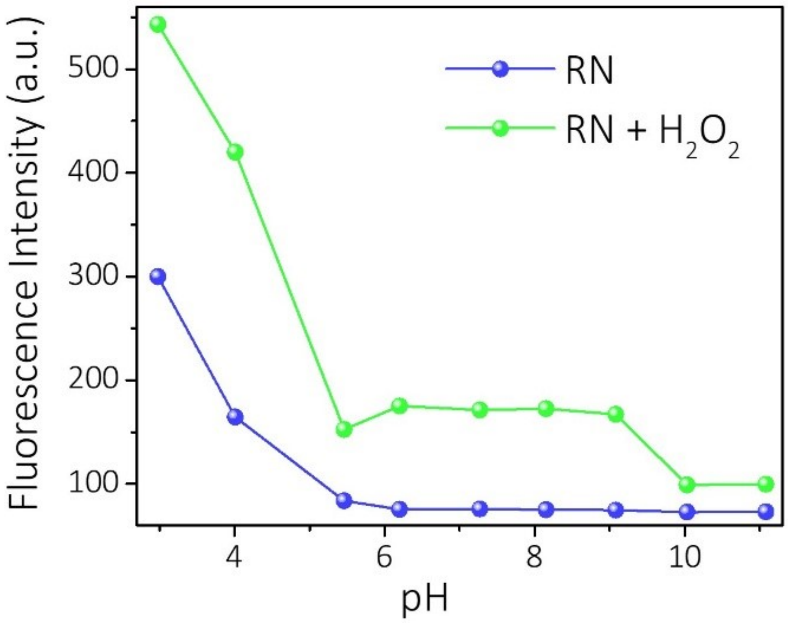

Figure S23: Effect of pH on the fluorescence intensity of 10 µM of RN before and after reaction with 500 µM of H_2O_2. The pH solutions were prepared using PBS buffer.

Figure S24: The vials containing RN (left) and RN+H_2O_2 (right) were kept in a UV inspection cabinet and an image was captured by a smartphone (Samsung Galaxy F13) under white light (λ_{ex}= 520 nm).

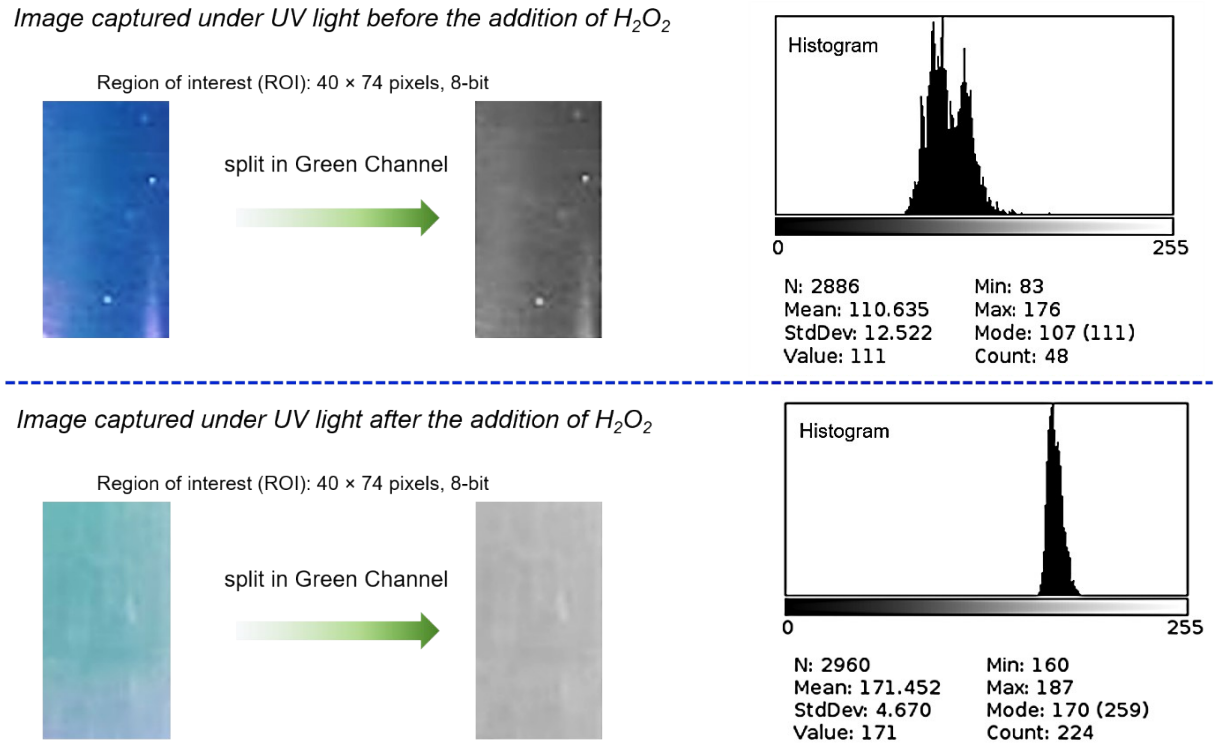

Figure S25: Green colour intensity analysis of captured images using ImageJ. Images captured by a smartphone under UV light irradiation.

Table S1: Some existing probes along with the newly reported probe RN

Probe	Recognition site	LOD	Response time	Application	Ref.
GW-1	Pentafluoro benzene	–	~30 min	–	[5]
Probe (mentioned as 3a)	Acetyl	0.57 µM	15 min	Milk detection and fluorescence imaging of HepG-2 cells and zebrafish	[6]
3c	Acetyl	0.35 µM	20 min	Milk detection and fluorescence imaging of HepG-2 cells and zebrafish	[6]
CNBE	Borate ester	1.35×10^{-6} M	30 min	exogenous and endogenous H_2O_2 in living cells and living animals by ratiometric fluorescence imaging	[7]
PR1 PF1 PX1	Boronate	~100–200 nM	30 min	Monitoring H_2O_2 in living cells, including hippocampal neurons	[8,9]
RN	–	0.67 ppm	~2 min	Milk detection and monitoring H_2O_2 generation in a diabetic L929 skin cell line and diabetic mice liver tissue	This work

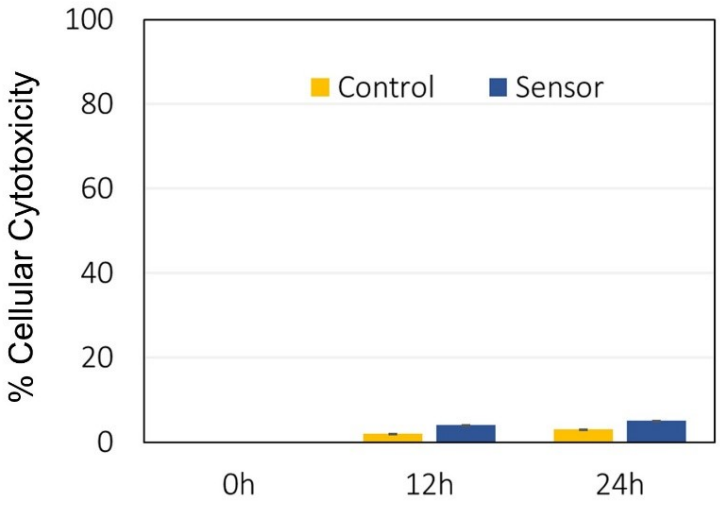

Figure S26: Graphical representation of the % cellular cytotoxicity of RN.

References

1 Y. Huang, P. Zhang, M. Gao, F. Zeng, A. Qin, S. Wu and B. Z. Tang, *Chem. Commun.*, 2016, **52**, 7288–7291.

2 G. Chen, F. Song, J. Wang, Z. Yang, S. Sun, J. Fan, X. Qiang, X. Wang, B. Dou and X. Peng, *Chem. Commun.*, 2012, **48**, 2949.

3 Y. Kong, R. Wu, X. Wang, G. Qin, F. Wu, C. Wang, M. Chen, N. Wang, Q. Wang and D. Cao, *RSC Adv.*, 2022, **12**, 27933–27939.

4 J. Hu and C. Zhang, *Anal. Chem.*, 2013, **85**, 2000–2004.

5 J. Su, S. Zhang, C. Wang, M. Li, J. Wang, F. Su and Z. Wang, *ACS Omega*, 2021, **6**, 14819–14823.

6 T. Peng, S. Ye, R. Liu and J. Qu, *Spectrochim. Acta Part A Mol. Biomol. Spectrosc.*, 2023, **297**, 122757.

7 K. Xu, L. He, X. Yang, Y. Yang and W. Lin, *Analyst*, 2018, **143**, 3555–3559.

8 E. W. Miller, A. E. Albers, A. Pralle, E. Y. Isacoff and C. J. Chang, *J. Am. Chem. Soc.*, 2005, **127**, 16652–16659.

9 M. C. Y. Chang, A. Pralle, E. Y. Isacoff and C. J. Chang, *J. Am. Chem. Soc.*, 2004, **126**, 15392–15393.